Nucleic Acids Research Advance Access published September 13, 2011

Nucleic Acids Research, 2011, 1–11
doi:10.1093/nar/gkr722

The biogenesis and characterization of mammalian microRNAs of mirtron origin

Christopher R. Sibley[1], Yiqi Seow[1,2], Sheena Saayman[3], Krijn K. Dijkstra[1], Samir El Andaloussi[1], Marc S. Weinberg[1,3] and Matthew J. A. Wood[1,*]

[1]Department of Physiology, Anatomy and Genetics, University of Oxford, South Parks Road, Oxford, OX1 3QX, UK, [2]Molecular Engineering Laboratory, Science and Engineering Institutes, A*STAR, Singapore and [3]Antiviral Gene Therapy Research Unit, Department of Molecular Medicine and Haematology, University of Witwatersrand, Johannesburg, South Africa

Received January 5, 2011; Revised and Accepted August 22, 2011

ABSTRACT

Mirtrons, short hairpin pre-microRNA (miRNA) mimics directly produced by intronic splicing, have recently been identified and experimentally confirmed in invertebrates. While there is evidence to suggest several mammalian miRNAs have mirtron origins, this has yet to be experimentally demonstrated. Here, we characterize the biogenesis of mammalian mirtrons by ectopic expression of splicing-dependent mirtron precursors. The putative mirtrons hsa-miR-877, hsa-miR-1226 and mmu-miR-1224 were designed as introns within eGFP. Correct splicing and function of these sequences as introns was shown through eGFP fluorescence and RT–PCR, while all mirtrons suppressed perfectly complementary luciferase reporter targets to levels similar to that of corresponding independently expressed pre-miRNA controls. Splicing-deficient mutants and disruption of key steps in miRNA biogenesis demonstrated that mirtron-mediated gene knockdown was splicing-dependent, Drosha-independent and had variable dependence on RNAi pathway elements following pre-miRNA formation. The silencing effect of hsa-miR-877 was further demonstrated to be mediated by the generation of short anti-sense RNA species expressed with low abundance. Finally, the mammalian mirtron hsa-miR-877 was shown to reduce mRNA levels of an endogenous transcript containing hsa-miR-877 target sites in neuronal SH-SY5Y cells. This work confirms the mirtron origins of three mammalian miRNAs and suggests that they are a functional class of splicing-dependent miRNAs which are physiologically active.

INTRODUCTION

Mirtrons, which were recently discovered and characterized in invertebrates, are novel cellular RNA interference (RNAi) effectors generated via a non-classical miRNA pathway (1,2). In canonical miRNA processing, Drosha initially cleaves mono- or poly-cistronic primary-miRNA (pri-miRNA) transcripts into precursor-miRNA (pre-miRNA) hairpins in the nucleus. The recognition sequence for processing appears to be a hairpin structure with ~33-bp stem and terminal loop flanked by un-paired nucleic acid sequences. The Drosha/DGCR8 microprocessor complex recognizes the flanking regions merging into the base of the stem and cuts the stem–loop ~11 nt in to produce the shortened pre-miRNA (3). In contrast, mirtrons were identified in small RNA libraries of invertebrates as small RNA species that clustered at the outer edge of short introns, with un-paired flanking sequences immediately adjacent to the splice junctions (1). Based on these observations splicing, rather than Drosha cleavage, is expected to be responsible for defining the ends of the pre-miRNA hairpin, with complementary sequences at the 5′- and 3′-ends of the intron allowing hairpin formation (1,2).

First reported in *Drosophila melanogaster* and *Caenorhabditis elegans*, experimental evidence to support the existence, splicing dependence and function of mammalian mirtrons is lacking. However, several lines of evidence suggest that mammalian mirtrons are likely to be produced as functional pre-miRNA precursors. Short RNA species corresponding to predicted mirtrons have been identified in mammalian small RNA libraries, some

*To whom correspondence should be addressed. Tel: +44 1865 272419; Fax: +44 1865 272420; Email: matthew.wood@dpag.ox.ac.uk

The authors wish it to be known that, in their opinion, the first two authors should be regarded as joint First Authors.

of which show cross-species conservation (4). These are likely to be processed independently of Drosha since the terminal nucleotides located towards the base of predicted hairpin stems represent the first or last nucleotides of intronic regions. These putative mirtrons, which lack extended hairpin features, do not form canonical Drosha substrates (3,4). Furthermore, ablation of the Drosha/DGCR8 microprocessor complex has a less severe phenotype than Dicer depletion in mouse embryonic stem cells, suggesting the existence of microprocessor-independent miRNAs in these cells (5). This was confirmed by deep sequencing from these two populations of cells, which reveal a subset of processed miRNAs in DGCR8 silenced cells that are located within referenced short introns and that are analogous to the mirtrons of *D. melanogaster* and *C. elegans* (1,2,5). However, additional pleiotropic effects of both Dicer and Drosha may also be responsible for this phenotype (6). Finally, the observation that some predicted mirtrons appear restricted to individual mammalian orders, for example the exclusively primate miR-1226, implies recent evolutionary origins and suggests that the mirtron biogenesis of miRNAs might be a mechanism in which new miRNA species can be introduced readily into gene regulatory pathways and subsequently have significant involvement in evolutionary diversification (4).

In this study, we demonstrate that mammalian mirtrons are functional RNAi effectors through the ectopic expression of mirtron precursors embedded as artificial introns within the coding region of eGFP. We show that functional mammalian mirtrons are capable of splicing-dependent silencing, are independent of Drosha processing, while dependence on the remainder of the RNAi pathway is variable. Moreover, we provide evidence of the functional activity of mirtrons by showing that hsa-miR-877 (miR-877) is able to reduce mRNA levels of an endogenous transcript containing seed-matched target sites for miR-877 in dopaminergic SH-SY5Y neuronal cells. These results provide the first experimental verification for the existence of the splicing-dependent mammalian miRNAs termed mirtrons.

MATERIALS AND METHODS

Constructs

All sequences used can be found in Supplementary Table S1.

For mirtron constructs, two fragments of eGFP were amplified by polymerase chain reaction (PCR) from pEGFP-C1 (Clontech, CA, USA) with the following primers (1st set: 5′-AGATCCGCTAGCGCTACCGGTC-3′ and 5′-GTCTACTCGAGAAGACTACTTGAAGAAGA TGGTGCGC-3′; 2nd set: 5′-GTCTTCTCGAGAAGACT TGACGACGGCAACTACAAGA-3′ and 5′-ATCGAAG CTTACTTGTACAGCTCGTCCAT-3′). The fragments were digested with restriction enzymes NheI/XhoI and XhoI/HindIII (NEB, MA, USA), respectively, and ligated back into the pEGFP-C1 vector, to create an EGFP transcript with two BbsI restriction sites between the 5′-TCTT CAAG/GACGACGG-3′ exon splice junction to form the pEGFP-Mirt plasmid. Subsequently, all mirtron inserts described in this article were made by ligating complementary primers (Sigma Genosys, UK) with a 5′-CAAG overhang on the sense strand and 5′-CGTC on the antisense in to a BbsI-digested pEGFP-Mirt plasmid.

pre-miRNA expression plasmids were designed with mirtron stem–loops being transcribed of a U6 promoter. PCR was performed with Pol-III U6 promoter as template and pre-miRNA as 3′ primer as follows: U6F 5′-ATCGGG CCCGTCGACAAGGTCGGGCAGGAAGAGGGCCT-3′; U6R 5′-AAAAAA-Antisense-TGGGTCAGG-Sense-GGTG TTTCGTCCTTTCCACAA-3′. PCR products were TA-cloned into the pGEM-T Easy vector (Promega) to generate pol-III expressed pre-miRNA plasmids. The miR-877 sponge was created in the same manner but with six consecutive FXR2 target sequences for miR-877 incorporated in replace of the hairpin sequence. Lentiviral constructs with conditionally expressed Drosha or non-specific shRNAs were a kind gift of Dr L. Aagaard.

Pri-miRNA-30-based expression plasmids were synthesized as previously outlined (7). Briefly, complementary oligonucleotides containing both anti-sense and sense strands separated by the miR-30 loop were annealed together and subcloned into the miR-30 pri-miRNA transcript under control of the U6 promoter using BfuA1 restriction sites. Pri-miRNA-122 constructs were a kind gift of Dr Abdullah Ely (8).

Target sequences of mirtrons used in the luciferase assay were synthesized as annealed complementary primers and ligated into psiCheck2.2 vector (Promega, USA) with XhoI and NotI restriction sites.

Human exportin-5 was cloned into peGFP-C1 downstream of eGFP with BspEI and XhoI, with the start codon beginning immediately after BspEI to produce pEGFP-XPO5.

Cell culture, transfections and luciferase assays

HEK-293 cells (ATCC, CRL-1573) and SH-SY5Y cells (ATCC, CRL-2266) were cultured in DMEM supplemented with 10% FCS. For transfection, cells were grown in 24-well plates to 80% confluence and transfected with Lipofectamine 2000 (Invitrogen, USA) according to manufacturer's instruction. All mirtron, shRNA and target plasmid constructs were transfected at a concentration of 500 ng/ml in HEK-293 cells unless otherwise stated. HEK-293 cells were harvested 2 days after transfection unless stated otherwise and probed for luciferase activity using dual-luciferase reporter assay system (Promega, USA) and Wallac-Victor 2 plate reader as per manufacturer's instructions. Ratios of renilla luciferase:firefly luciferase were obtained and normalized to specific construct controls utilizing the same promoter. Dominant negative Drosha expression plasmid was a kind gift from Dr V. Narry Kim (Seoul University) (9). Dominant negative Drosha was transfected at a concentration of 500 ng/ml 24 h prior to transfection of experimental constructs each at concentrations of 200 ng/ml. Transfection of mirtrons into SH-SY5Y cells was carried out at 2 μg/ml and harvesting for protein and RNA carried out 4 days post-transfection. For conditional expression of shRNAs

from lenti-viral constructs, cells were grown in the presence of 5 μg/ml doxycyclin for 8 days prior to transfection, and maintained in selection media for the duration of experiments.

GFP quantification

peGFP-Mirt transfected HEK-293 cells were lysed at 48 h post-transfection and protein content determined using the micro BCA protein assay (Pierce Biotechnology, USA). Fifty microgram of protein was assayed for GFP fluorescence using a plate reader. Background fluorescence determined from cells transfected with target alone was subtracted.

RT–PCR and RT-qPCR

peGFP-Mirt transfected HEK-293 cells were lysed at 48 h post-transfection and RNA harvested using the Trizol protocol (Invitrogen, USA). Reverse transcription was performed on 500 ng of RQ1 DNase treated (Promega, USA) RNA using an expand reverse-transcriptase kit (Roche, UK) and sequence specific reverse primer. PCR reactions were performed using primers flanking the intronic region inserted into GFP (5′-TCTTCAAGTCC GCCATGCC-3′ and 5′-TGTCGCCCTCGAACTTCA C-3′). PCR products were visualized on a 3% agarose gel. For real-time PCR of target mRNAs, 1 μg of total RNA was reverse transcribed with random hexamers using the Precision Reverse Transcription kit (PrimerDesign, UK) as per manufacturer's instructions. Realtime PCR was performed with 25 ng of cDNA using Precision Mastermix (PrimerDesign, UK). For small RNA qPCR, 10 ng of total RNA was reverse transcribed with sequence-specific stem–loop primers and the Taqman miRNA Reverse Transcription kit (Applied Biosystems, USA) according to manufactures protocol. Realtime PCR was performed on 1 ng of cDNA using Taqman Universal PCR Master Mix and custom Taqman probes (Applied Biosystems, USA).

RNAi pathway saturation

Saturation of Exportin-5 and Dicer was carried out as previously reported using adenoviral associated RNA 1 (VA1) (10) using the pAdVantage vector (Promega, USA) expressing both VA1 and VA2. Luciferase targets and respective shRNA/mirtron constructs were transfected each at a constant concentration of 500 ng/ml and luciferase assays performed 48 h post-transfection. Concentrations of pAdVantage were subsequently varied from 0 to 2 μg/ml in individual experiments, with the total DNA transfected maintained constant at 3 μg/ml by co-transfection with a stuffer plasmid at appropriate concentrations. Results are normalized to the luciferase ratio determined for the non-targeting control construct for each individual experiment in the absence of pAdVantage.

Northerns/small RNA detection

Thirty micrograms of total RNA extracted from HEK-293 cells 48 h post-transfection was resolved on urea denaturing 15% polyacrylamide gels and blotted onto nylon membranes. Decade Marker (Ambion, USA) was prepared according the manufacturer's instructions and run alongside the cellular RNA. Blots were hybridized to DNA oligonucleotides complementary to regions spanning the target antisense sequences of the hairpins. Probes were labelled at their 5′-ends using [γ-^{32}P] ATP with T4 Polynucleotide kinase then purified using standard procedures. Analysis was carried out using a FLA-7000 phosphorimager (Fujifilm, Japan). Oligonucleotide sequences used as probes were: mir-877—5′ CCCCTGCGCCATCTCCTCTAC; miR-1224—5′ CTCCACCTCCCCAGTCCTCAC.

To perform 3′-rapid amplification of cDNA ends (RACE) of miR-877 mature species, 1 μg of total RNA was poly-A tailed and reverse-transcribed with the NCode Vilo miRNA cDNA synthesis kit (Invitrogen, USA) as per manufacturer's instructions. cDNA products were subject to PCR using a universal reverse primer and miR-877 specific forward primer (5′ GTAGAGGAGATGGCGC AGG 3′). Product were visualized on a 3% agarose gel and additionally TA cloned into the pGem T-Easy vector (Promega, UK), transformed and individual colonies sequenced (Geneservice, UK).

High-throughput sequencing

HEK cells were grown in 24-well plates to 80% confluence and transfected with 500 ng of each mirtron. Small RNA libraries were prepared with the 'Small RNA v1.5 Sample Prep Kit' following the manufacturer's instructions (Illumina). Briefly, total RNA was isolated from each transfection by Trizol extraction and pooled. The RNA was ligated with 3′ RNA adaptor modified to target small RNAs with 3′ hydroxyl groups, and then with 5′ RNA adaptor. Reverse transcription followed by PCR was performed to select for adapter ligated fragments and double-stranded DNA libraries were size selected by PAGE purification (6% TBE PAGE). Libraries were sequenced on a Genome Analyzer IIx for 36 cycles following manufacturer's protocols. The image analysis and base calling were done using Illumina's GA Pipeline. Adapters were trimmed with Biopieces remove_adapter script and remaining sequences were aligned against full-length mirtron hairpins.

Western blotting

Cells were lysed at 48 h post-transfection, protein content determined using the micro BCA protein assay (Pierce Biotechnology, USA), and 25 μg run on 10% SDS–PAGE gels. For Drosha western detection, blots were probed with a rabbit polyclonal antibody to Drosha at a 1:1000 dilution. Blots were stripped and re-probed with mouse monoclonal to GAPDH at 1:20 000. Goat anti-rabbit secondary antibodies (Chemicon, USA) were used at a 1:10 000 dilution, and goat anti-mouse secondary at 1:10 000. All antibodies were purchased from Abcam (Abcam, USA) unless otherwise stated.

Statistical analysis

Statistical significance between control and experimental values was determined using Student's *t*-test (paired, two

tailed). All data are expressed as means ± SD unless otherwise stated.

RESULTS

miR-877, miR-1224 and miR-1226 are functional mammalian introns

To test whether predicted mammalian mirtrons are functional introns, the 86 nt human sequence of the conserved mammalian miRNA, miR-877, the 85 nt murine sequence of the conserved miRNA, miR-1224 or the 75 nt sequence of the primate-specific miRNA, miR-1226, were placed into a modified expression plasmid, peGFP-Mirt, as introns within the eGFP open reading frame (ORF; Figure 1A and Supplementary Figure S1). Variants of the putative mirtron sequences of miR-877 (mirt-miR-877), miR-1224 (mirt-miR-1224) and miR-1226 were generated in which mutations were made to key regulatory sequences required for splicing (Figure 1B and Supplementary Figure S1). These included changes to the predicted branch point sequence within a CAGAC motif in the loop region of miR-877 (mirt-miR-877BP), and changes to one or both of the invariant splice site recognition sequences at the 5′- or 3′-ends of the intron for all miRNAs (mirt-miR-877US, mirt-miR-877DUS, mirt-miR-1224DUS, mirt-miR-1226US). Although, attempts were made to identify the branch-point of miR-1224 and miR-1226 by making constructs with changes at putative branch point sequences, none of these mutations abolished splicing and were omitted for these putative mirtrons. The branch point is indispensible for the splicing reaction and an A residue acts as the site of 2′–5′ diester linkage in formation of intermediate branched lariats (11). The terminal 5′ splice site recognition sequence of GU and the 3′ splice-site recognition sequence of AG are highly conserved across introns such that changes to either of these regions is likely to interfere with splice junction determination (11). A final construct was generated in which the predicted mature sequence of miR-877 was scrambled (mirt-miR-877Scr) (Figure 1B)

Expression of mirt-miR-877, mirt-miR-1224 and mirt-miR-1226 in HEK-293 cells resulted in eGFP fluorescence, which is indicative for successful splicing, as did incorporation into the peGFP-Mirt vector of a comparable length (91 nt) control derived from NADH-coenzyme Q reductase intron 6 (NAD intron) which lacks hairpin-forming potential (Figure 1C and Supplementary Figure S1). Whereas mirt-miR-877Scr also spliced successfully, mutations made in mirt-miR-877BP, mirt-miR-877US and mirt-miR-877DUS abrogated eGFP fluorescence. Quantification of eGFP shows that fluorescence levels generated by mirt-miR-877 and mirt-miR-877Scr were 21% and 60% of the NAD intron, respectively (Figure 1D), indicating that miR-877 is less efficient as an intron compared to the NAD intron and implying that sequence changes in mirt-miR-877Scr improve splicing efficiency. The incomplete splicing of mirt-miR-877 in this system could represent a consequence of placing this intron outside of its natural sequence context, or alternatively it may reflect a recent evolution of this sequence as

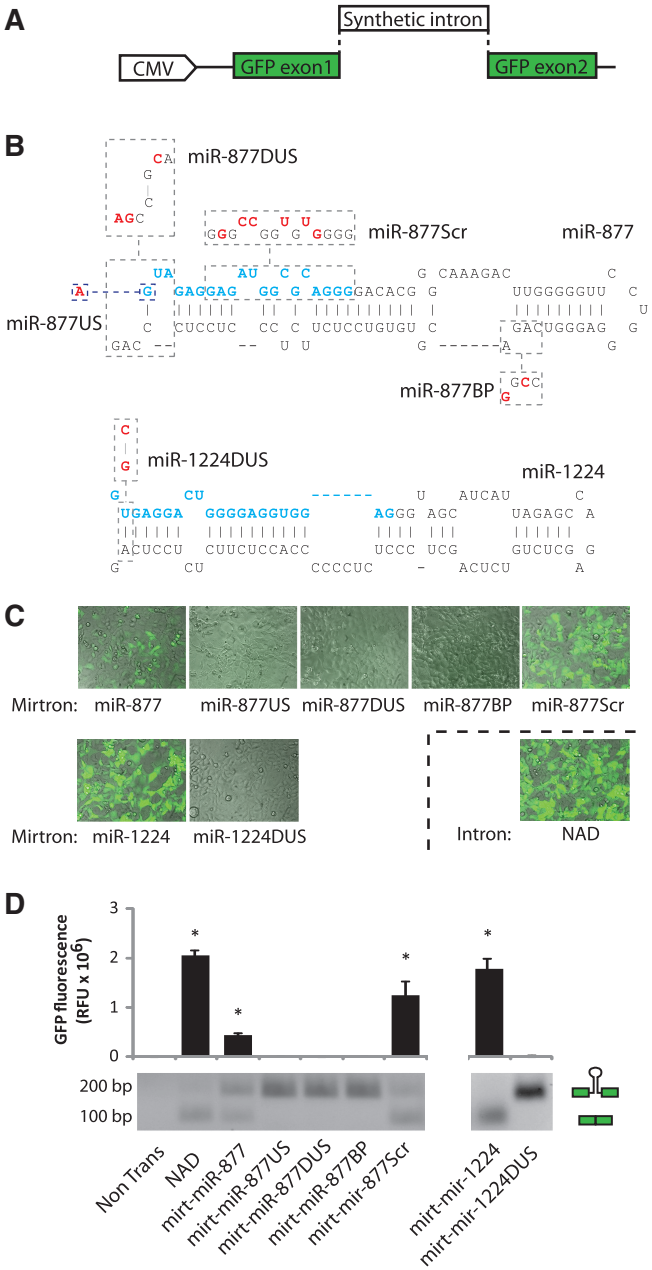

Figure 1. miR-877 and miR-1224 are functional mammalian introns. (**A**) Putative mirtrons were studied by inserting appropriate sequences as introns within an eGFP transcript. (**B**) Predicted mirtron alignments for miR-877 and miR-1224 sequences incorporated into the pMirt vector. Variants with modifications made to splicing regulatory sequences are indicated by dashed boxes. US = unspliceable, DUS = double unspliceable, BP = Branch-point, Scr = Scrambled. Blue and red nucleotides represent the guide sequence and modified nucleotides, respectively. (**C**) Representative fluorescent microscopy images of different mirt-miR-877 and mirt-miR-1224 variants 48 h after transfection in HEK-293 cells. NAD represents a control intron of comparable length to miR-877 and miR-1224 with no hairpin-forming potential. (**D**) Upper panel—Quantification of eGFP fluorescence following expression of mirt-miR-877 and mirt-miR-1224 variants in HEK-293 cells. Values represent mean fluorescent ±SD from $n = 3$. $^*P < 0.05$ relative to non-transfected cells. Lower panel—RT–PCR with intron-spanning primers following expression of miR-877 and miR-1224 variants in HEK-293 cells.

an intron. Mirt-miR-1224 was also splicing-competent and successfully produced 78% of the fluorescence of the control NAD intron, while mutations made to the 5′- and 3′-splice sites in mirt-miR-1224DUS resulted in no detectable eGFP fluorescence (Figure 1C and D). This suggests miR-1224 was more efficient as an intron than miR-877, perhaps because of a longer poly-pyrimidine tract in its 3′ arm which is necessary for proper splicing. Lastly, mirt-miR-1226 spliced to 45% of the level of the NAD intron, and this was abrogated by 5′ splice site mutations in mirt-miR-1226US (Supplementary Figure S1).

To demonstrate that eGFP fluorescence correlates with intron removal, RT–PCR was performed using intron-spanning primers on total RNA from cells transfected with mirt-miR-877 and mirt-miR-1224 variants (Figure 1D). The ratio of un-spliced to spliced transcripts, represented by large and small transcripts, respectively, confirms results seen with eGFP quantification. More un-spliced transcript was produced compared to spliced transcript for mirt-miR-877 (63% versus 37%, respectively), and less un-spliced transcript was produced than spliced transcript for mirt-miR-877Scr (37% versus 63%, respectively). In contrast, no spliced transcript was observed in eGFP-negative variants of mirt-miR-877. The enhanced eGFP production of mirt-miR-1224 relative to mirt-miR-877 was also seen with RT-PCR, with near complete (88%) spliced transcript produced for mirt-miR-1224 (Figure 1D). Together the results demonstrate that miR-877 and miR-1224 possess necessary sequence constraints to be spliced from a co-expressed mRNA transcript.

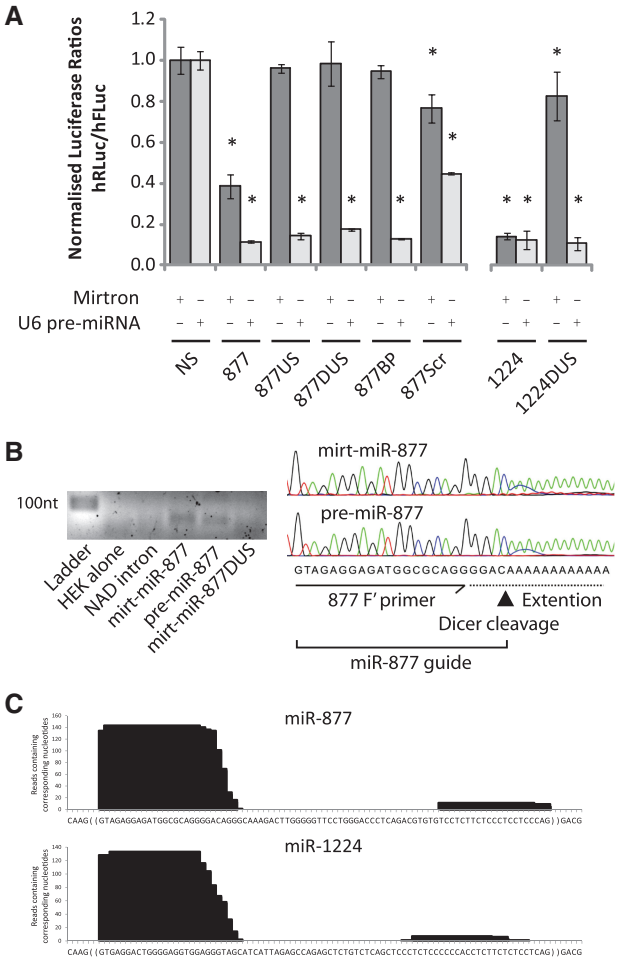

Figure 2. miR-877 and miR-1224 are splicing-dependent mammalian mirtrons processed into small RNA species. (**A**) Dual-luciferase reporter assays showing knockdown of a complementary miR-877 target or miR-1224 target following co-transfection with indicated mirtron (dark bars) and pre-miRNA control (light bars) variants. Values represent mean ratios of *Renilla*: Firefly luciferase ±SD from $n = 6$. Mirtron variants are normalized to cells transfected with the NAD variant. Pre-miRNA variants are normalized to cells transfected with a non-specific U6 pre-miRNA hairpin. $^{*}P < 0.05$ relative to respective normalizing control. (**B**) Upper panel—3′ RACE RT–PCR of total RNA from HEK-293 cells transfected with NAD construct or mirtron/pre-miRNA variants of miR-877 using a miR-877 specific forward primer. Lower panel—Sequencing of 3′ RACE RT-PCR products identifies Dicer cleavage sites. (**C**) 18–25 nt small RNAs were extracted by polyacrylamide gel isolation from total RNA of HEK cells transfected with equimolar amounts of miR-877 and miR-1224 each as introns within separate eGFP mRNAs. Linkers were added to both ends of the RNA for RT–PCR amplification before deep sequencing using an Illumina Genome Analyzer. Sequences highly matched to any part of miR-877 or miR-1224 hairpin were identified and the incidence of each nucleotide in the sequenced small RNAs was plotted against miR-877 or miR-1224 sequences.

miR-877, miR-1224 and miR-1226 are splicing-dependent mammalian mirtrons

The miRNA derived from the 5′-arm of miR-877 is enriched in small RNA libraries compared to that derived from the 3′-arm, suggesting that the 5′-arm harbours the dominant miRNA species (4). Similarly, the 5′-arm of miR-1224 produces the dominant species in small RNA libraries (4,12). In contrast the 3′-arm of miR-1226 is expected to be processed into the dominant miRNA species (4). Thus, fully complementary targets to the 5′-arm of both miR-877 and miR-1224, and the 3′-arm of miR-1226 were inserted in the 3′-UTR of *Renilla* luciferase gene in a dual-luciferase reporter vector. Ratios of *Renilla* luciferase to constitutively expressed Firefly luciferase were used to assess knockdown efficiency.

Expression of mirt-miR-877 alongside its target resulted in knockdown of 60% ($P = 0.001$), while this silencing effect was abolished by splicing-deficient mutants (Figure 2A). This implies that silencing had been achieved with mirt-miR-877 in a splicing-dependent manner. To eliminate the possibility that the mutations introduced into splicing-deficient variants directly affected knockdown of the target, U6-driven pre-miRNA controls were made, which corresponded to the sequences of putatively spliced mirtron variants. Expression of each variant alongside the miR-877 target sequence demonstrated no effect on the silencing ability relative to the respective wild-type pre-miRNA control. This was despite single nucleotide mismatches to the miR-877 target sequence at the 5′-end of pre-miR-877US and pre-miR-877DUS guide strands, and minor weakening of the predicted pre-miRNA hairpins of each variant (Figure 2A). This confirmed that the introduced mutations abrogated silencing by

inhibiting splicing rather than by producing pre-miRNA substrates that inefficiently enter downstream RNAi events. Reduced levels of silencing were seen with both mirtron and pre-miRNA scrambled constructs when compared to wild-type constructs, thus confirming that knockdown by mirt-miR-877 was a sequence-specific effect (Figure 2A). A target complementary to the 3′-arm of miR-877 was not silenced by any construct, which corroborates deep sequencing data that the 5′-arm miRNA of miR-877 is preferentially selected (Supplementary Figure S2). Collectively, these data are consistent with miR-877 acting as a splicing-dependent RNAi effector which derives an antisense species from its 5′-arm, and imply that miR-877 has mirtron origins.

Mirt-miR-1224 and mirt-miR-1226 also silenced corresponding dual-luciferase targets by 87% ($P < 0.001$) and 35% ($P = 0.002$), respectively, with silencing inhibited in both cases by mutations made to splice sites (Figure 2A and Supplementary Figure S1). The weak silencing by the mirt-miR-1224DUS mutant is likely to be an artefact rather than a Drosha-dependent effect (Figure 2A). Silencing by miR-1224 and miR-1226 pre-miRNA variants subsequently confirmed that mutations affect splicing rather than silencing efficiency of the antisense species (Figure 2A and Supplementary Figure S1), and collectively the data verifies the splicing-dependent mirtron origins of both miR-1224 and miR-1226. In addition, silencing by mirt-miR-1224 was equal to that of the equivalent pre-miR-1224 control (Figure 2A). This shows that mirtrons can silence as effectively as independent pre-miRNA precursors, and this result may have implications for development of synthetic mirtrons.

miR-877 is processed to small RNA species that correspond to the predicted guide strand

To confirm that RNAi was responsible for the silencing effect of these mirtrons, we sought to detect processed small RNA species of mirt-miR-877 and mirt-miR-1224 pre-miRNA and mirtron variants with northern blots using standard or locked nucleic acids (LNA)-based probes. The mature miRNA species could not be detected for any of these constructs while pre-miRNA precursors could be detected for all constructs except mirt-miR-877. This suggests that the hairpin processed from mirt-miR-877 is in low abundance and escapes detection. This is likely since precursors of the pre-miR-877 control were detected (Supplementary Figure S3). Interestingly, however, the processed pre-miRNA species detected for the mirt-miR-1224 variant was expressed ~22.5-fold lower than the pre-miR-1224 control despite comparable levels of silencing (Supplementary Figure S3). Mirtrons therefore appear capable of directing comparable levels of silencing to a U6-expressed pre-miRNA, despite much weaker levels of precursor expression. This could be indicative of a controlling step in mirtron biogenesis which may act to limit the accumulation of potentially toxic pre-miRNA-like hairpins in the cell in a manner equivalent to that seen in Drosha processing of pri-miRNAs (13,14).

An alternative 3′-RACE approach was devised to detect mirt-miR-877 small RNA species in which a poly-A tailing and first strand-synthesis step was followed by PCR with a mature miR-877 sequence-specific primer and a universal primer. Bands of expected size were detected for both mirt-miR-877 and pre-miR-877, but not for the NAD intron and mirt-miR-877DUS (Figure 2B). The miR-877 specific forward primer was designed to reveal precise position of Dicer cleavage by extension through the guide strand/polyA junction. Cloning and sequencing of the products revealed sequences corresponding to the predicted miR-877 mature sequence for both mirtron and pre-miRNA control variants (Figure 2B). The results confirm that small RNA species are being processed and generated from miR-877 precursor constructs of mirtron origin.

Finally, deep sequencing following enrichment of small RNA species was performed in HEK-293 cells transfected with mirt-miR-877, mirt-miR-1224 and mirt-miR-1226. Sequence reads corresponding to the predicted mature species of each mirtron were detected (Figure 2C and Supplementary Figure S1). Interestingly, despite similar amounts of each construct being transfected in each experiment, it can be seen that miR-1226 displays a much lower number of read counts, likely indicating inefficient processing from this construct and potentially explaining its poor silencing ability. When taken together with the results in Figure 2A, the data confirm that miR-877, miR-1224 and miR-1226 are splicing-competent mirtrons capable of complementary target silencing in an RNAi-like manner.

Mammalian mirtrons are Drosha independent

To examine the role of Drosha in mirtron-mediated RNAi, HEK-293 cells were transduced with a lentivirus containing a Drosha-targeting shRNA (15), resulting in reduced Drosha expression by 66% relative to cells stably expressing a non-specific shRNA (Figure 3A). To first confirm that Drosha knockdown affected miRNA processing, pri-miR-30 and pri-miR-122 mimics were transfected with corresponding luciferase targets. Both pri-miR-30 mimics containing α-synuclein targeting guide strands and a miR-122 mimic containing an HBV targeting guide strand (8) showed significantly reduced levels of silencing of their respective fully complementary luciferase targets when the Drosha shRNA was expressed relative to the control shRNA (Figure 3B and Supplementary Figure S4). However, the de-repression of silencing by pri-miR-122/HBV and both α-synuclein pri-miR-30 mimics was not complete, indicating the presence of residual amounts of Drosha activity.

We next looked at the effects of Drosha silencing on miR-877 activity. As a separate Drosha-dependent control, we generated a pri-miR-30 mimic embedded with miR-877 guide sequence (pri-miR-30/877). Following shRNA-mediated silencing of Drosha, both the mirt-miR-877 construct and pre-miR-877 control retained the ability to silence the luciferase target to the same levels as those shown in the non-specific shRNA-expressing cells. In contrast, the pri-miR-30/877 construct presented

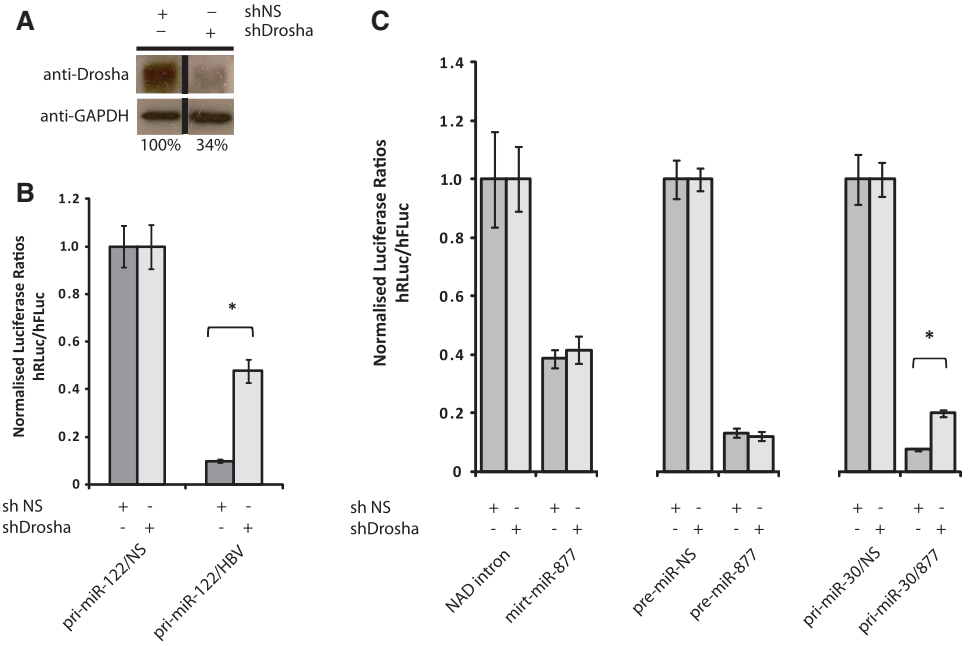

Figure 3. Mammalian mirtrons are Drosha independent. (**A**) Western blotting of protein lysates following transduction of HEK-293 cells with lentivirus expressing a non-specific control shRNA or Drosha targeting shRNA. (**B**) Dual-luciferase reporter assay showing knockdown of a HBV target sequence following co-transfection with an HBV-targeting pri-miR-122 mimic in the presence of a non-specific shRNA or Drosha-targeting shRNA. Values represent mean ratios of *Renilla*: Firefly luciferase ±SD from $n = 6$. Values are normalized to cells transfected with a non-specific pri-miR-122 mimic in the presence of the respective shRNA construct.*$P < 0.05$ relative to respective normalizing control. (**C**) Dual-luciferase reporter assay showing knockdown of a miR-877 target sequence following co-transfection with indicated mirt-miR-877, pre-miR-877 or miR-877 pri-miR-30 mimic in the presence of a non-specific shRNA or Drosha-targeting shRNA. Values represent mean ratios of *Renilla*: Firefly luciferase ±SD from $n = 6$. Mirtron variants are normalized to cells transfected with the NAD variant. Pre-miRNA variants are normalized to cells transfected with a non-specific U6 pre-miRNA hairpin. Pri-miRNA-30 mimics are normalized to cells transfected with a non-specific pri-miR-30 mimic. *$P < 0.05$ relative to respective normalizing control.

significantly reduced expression of the target (Figure 3C), with residual Drosha levels likely accounting for incomplete de-repression. The additional mirtrons, miR-1226 and miR-1224, were likewise unaffected by Drosha knockdown (Supplementary Figure S4).

Finally, silencing by mirt-miR-877 was unaffected by co-expression of a dominant negative Drosha construct (Tn Drosha) with mutations made to both RNase III domains (9). In contrast, silencing by the pri-miR-30/877 construct was significantly reduced from 86% to 69% ($P < 0.001$) (Supplementary Figure S4). It is clear that the unchanged silencing activity of mirt-miR-877 in both of these assays indicates that entry into the RNAi pathway by mammalian mirtrons is below the level of Drosha processing, corroborating the results associated with mirtrons in *D. melanogaster* (1).

Mammalian mirtrons have variable dependence on the canonical RNAi pathway downstream of Drosha

In invertebrates, the predicted alignments of mirtron pre-miRNA hairpins result in 2 nt overhangs at the 3′-end of mirtrons. This follows both the consensus termini preference of Drosha processing and the recognition signals for exportin-5-mediated export and Dicer binding (3,16,17). In contrast, most predicted mammalian mirtron alignments exhibit atypical overhangs at the base of the stem (4). Examples include single nucleotide overhangs at both the 5′- and 3′-ends (miR-1224), and 3 nt 5′ overhangs together with 2 nt 3′ overhangs (miR-1226). As such, it is unclear to what extent putative mammalian mirtrons are dependent on RNAi pathway elements following pre-miRNA formation.

In order to determine the dependence of mammalian mirtrons on processing steps downstream of Drosha cleavage, we saturated the canonical pathway using adenoviral associated RNA (VA1), a substrate for both Exportin-5 and Dicer (10). As expected, expression of competing VA1 successfully led to reduced silencing of the miR-877 target by the pre-miR-877 control in a concentration-dependent manner (Figure 4A). Transfection alongside mirt-miR-877 likewise leads to de-repression of the miR-877 target, suggesting that miR-877 mirtron is likely to be dependent on both Exportin-5 and Dicer (Figure 4B) and furthermore that the identity of Exportin-5 substrates may be less constrained than previously thought. Indeed, exogenous addition of Exportin-5 rescued the silencing ability of mirt-miR-877 in the presence of VA1, which suggests that at least part of the VA1 abrogation of silencing was due to reduced Exportin-5 availability (Supplementary Figure S5). It is expected that the increased silencing by mirt-miR-877 in the presence of Exportin-5 and VA1 relative to Exportin-5 alone is a result of VA1s ability to enhance transient protein expression leading to increased Exportin-5 availability (18).

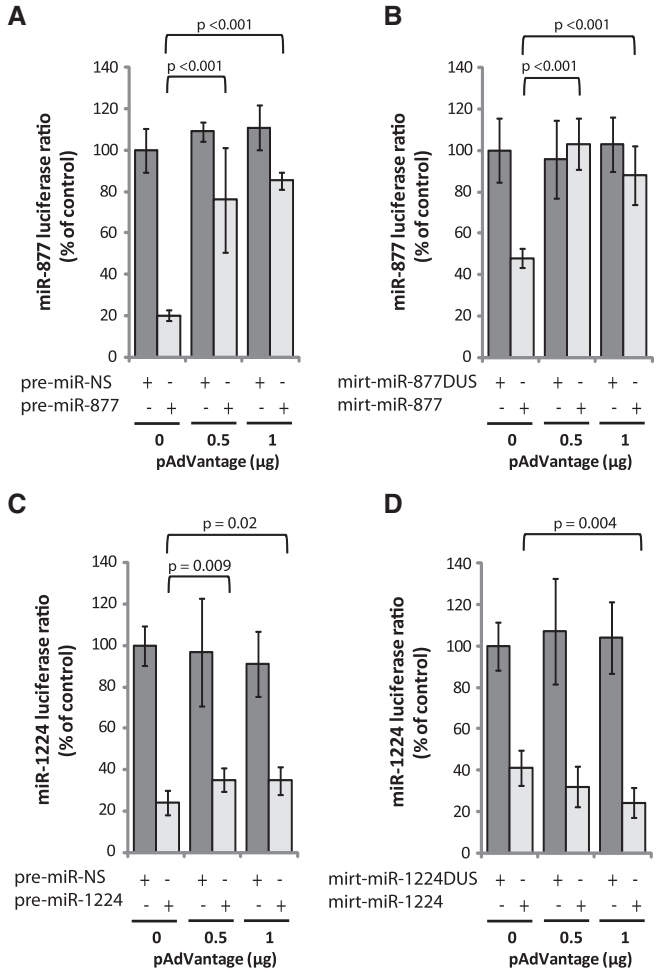

Figure 4. Mammalian mirtrons have variable dependence on the canonical RNAi pathway following pre-miRNA formation. (**A** and **B**) Dual-luciferase reporter assay showing knockdown of a miR-877 target sequence following co-transfection with indicated pre-miR-877 variants (A) or mirt-miR-877 variants (B) in the presence of increasing concentrations of VA1 expressed from the pAdvantage vector. Values represent mean ratios of *Renilla*: Firefly luciferase ±SD from $n = 6$. Pre-miRNA variants (A) are normalized to cells transfected with a non-specific U6 pre-miRNA hairpin and no pAdvantage vector. Mirtron variants (B) are normalized to cells transfected with mirt-miR-877DUS and no pAdvantage vector. (**C** and **D**) Dual-luciferase reporter assay showing knockdown of a miR-1224 target sequence following co-transfection with indicated pre-miR-1224 variants (C) or mirt-miR-1224 variants (D) in the presence of increasing concentrations of VA1 expressed from the pAdvantage vector. Values represent mean ratios of *Renilla*: Firefly luciferase ±SD from $n = 6$. Pre-miRNA variants (C) are normalized to cells transfected with a non-specific U6 pre-miRNA hairpin and no pAdVantage vector. Mirtron variants (D) are normalized to cells transfected with mirt-miR-1224DUS and no pAdVantage vector.

In contrast, attempts to saturate both pre-miR-1224 and mirt-miR-1224 variants with VA1 were unsuccessful (Figure 4C and D) and expression of exogenous Exportin-5 (Supplementary Figure S5) does not increase mirt-miR-1224 knockdown either. Both variants have single nucleotide overhangs at both the 5′- and 3′-ends of the hairpin and it is possible that this structural motif is not favoured by Exportin-5 and/or Dicer binding. In the presence of very high concentrations of Exportin-5, brought about by VA-1 expression, competition with canonical targets of Exportin-5 is reduced and miR-1224 can be a substrate for Exportin-5, leading to increased silencing (95%) (Supplementary Figure S5).

miR-877 silences the predicted seed-matched target FXR2 in neuronal SH-SY5Y cells

We next sought confirmation that mirtrons are physiologically relevant mammalian miRNAs. Microarray data indicates that the ATP-binding cassette subfamily F member 1 (ABCF1) transcript, within which miR-877 is the 13th intron, is expressed in the human dopaminergic SH-SY5Y cell line (19). Likewise, miRNA expression profiling implies that miR-877 is expressed in this cell line, albeit at low levels (∼1.1% of all miRNA species) (20). The expression of miR-877 in a neuronal cell line such as SH-SY5Y supports previous predictions that this is a primate-specific mirtron identified in small RNA libraries from brain tissue (4). We therefore identified nine high-scoring putative 3′-UTR targets of miR-877 using two miRNA target prediction algorithms (seven from targetscan, two from miranda), which were additionally expected to be expressed in this cell line (Supplementary Table S2). Short luciferase targets corresponding to the strongest predicted miR-877 3′-UTR target sites for each of these genes where generated and expressed alongside either mirt-miR-877 or the pre-miR-877 control in HEK-293 cells. Normalization to non-specific control constructs demonstrated that six of these targets were silenced in response to mirt-miR-877 and pre-miR-877 despite highly similar seed sequences across all targets (Figure 5A). These data imply that miR-877, like canonical miRNAs, is able to silence imperfectly matched target sequences with extensive base pairing across the seed region, while some of the identified target sequences may not be functional miR-877 target sites although this remains to be confirmed.

In order to confirm SH-SY5Y cells as a model cell line to study miR-877, RT–PCR and sequencing were first used to confirm removal of intron 13 in the ABCF1 mRNA transcript (Supplementary Figure S6). Guide strands of processed miR-877 were subsequently detected with qPCR in SH-SY5Y cell total RNA extract. However the miR-877 guide strand was in low abundance relative to both the small nucleolar RNA, RNU-24 and miR-16, which is in agreement with previous deep-sequencing data (Figure 5B and Supplementary Figure S6). Transfection of either a miR-877 targeting antagomir or a miR-877 sponge bearing seven sequential FXR2 target sequences driven off a U6 promoter were initially used to determine if de-repression of the FXR2 target could be detected. No change in protein or mRNA levels was seen and it is possible that the miRNA are too low in this cell line for any interaction to be detected. Recently, it was shown that ≥84% of miRNA targets demonstrate reductions in mRNA levels in the presence of the targeting miRNA (21). Therefore, to determine if this is true for miR-877 targets, mirt-miR-877 or the control NAD intron were overexpressed in SH-SY5Y cells. At 96 h post-transfection

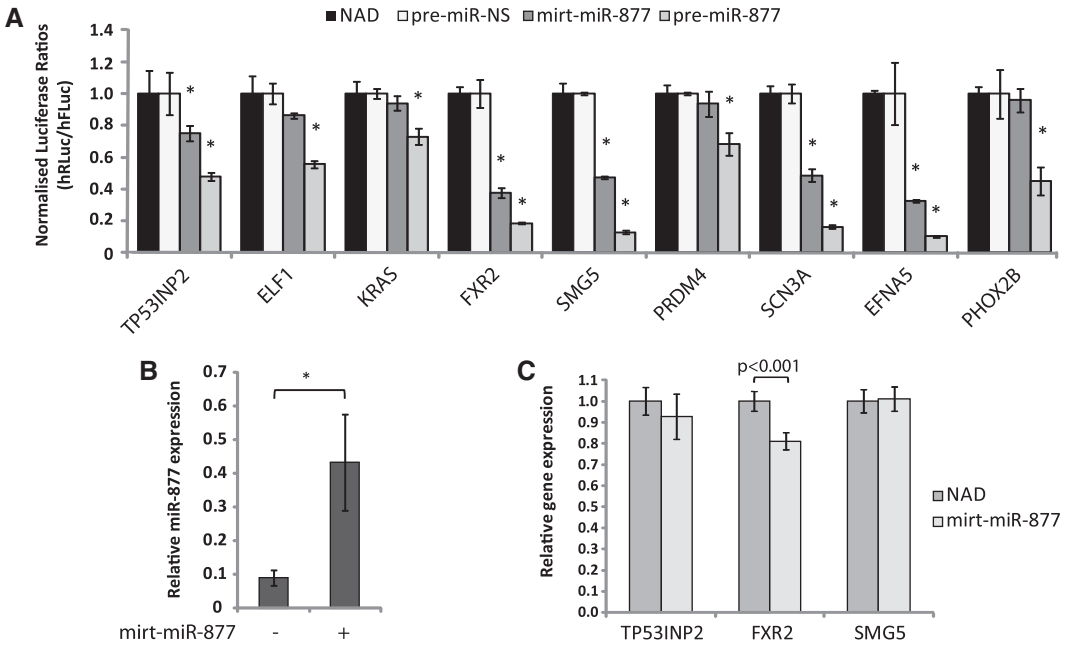

Figure 5. miR-877 silences the predicted seed-matched target FXR2 in neuronal SH-SY5Y cells. (**A**) Dual-luciferase reporter assay showing knockdown of predicted miR-877 target sequences following co-transfection with indicated mirt-miR-877 or pre-miR-877 variants. Values represent mean ratios of *Renilla*: Firefly luciferase ±SD from $n = 3$. For each unique target, mirtron variants are normalized to cells transfected the NAD variant and pre-miRNA variants are normalized to cells transfected with a non-specific U6 pre-miRNA hairpin. $*P < 0.05$ relative to respective normalizing control. (**B**) qPCR detection of miR-877 in SH-SY5Y cells in the presence or absence of mirt-miR-877. Values represent relative miR-877 expression normalized to RNU-24 expression using the $2^{-\Delta Ct}$ method and $n = 6$. (**C**) Relative expression of putative miR-877 target transcripts determined with RT–qPCR following transfection of SH-SY5Y cells with the NAD variant or mirt-miR-877. Values represent mean expression relative to β-actin expression ±SD using relative standard curve method and $n = 6$. Transcript levels in presence of mirt-mir-877 are normalized to cells transfected with the NAD variant.

qPCR revealed a 4.8-fold increase in miR-877 guide strand abundance when mirt-miR-877 was expressed relative to endogenous levels in the presence of the NAD intron (Figure 5B and Supplementary Figure S6). This change was lower than expected given the strong promoter, high transfection efficiency and extensive eGFP fluorescence seen. However, the data are in agreement with northern blots that low levels of miR-877 are processed from this construct. At this time point the transcript levels of FXR2 and other predicted miR-877 targets identified in luciferase assays were determined by qPCR. A significant 19% reduction ($P < 0.001$) in relative expression of the FXR2 transcript was detected in the presence of overexpressed mirt-miR-877 relative to the NAD intron, whereas additional targets failed to show any significant reduction (Figure 5C). This level of FXR2 target knockdown was additionally confirmed following transfection with the pre-miR-877 control construct (Supplementary Figure S7). Attempts to detect reduction of FXR2 protein levels by western blot were unsuccessful in transient transfection experiments, suggesting either a long half-life for this protein FXR2, or that more robust inhibition, perhaps with other miRNAs in conjunction, may be needed to induce functional knockdown. However, collectively the data confirms that an anti-sense species derived from miR-877 functionally interacts and is able to reduce mRNA transcripts of FXR2, but further characterization is needed to confirm FXR2 as an endogenous target of this mirtron.

DISCUSSION

Canonical mammalian miRNA biogenesis initially involves processing of long primary-miRNA transcripts by a microprocessor complex (3), yet recent evidence has demonstrated alternative methods of mature miRNA generation (1,22,23). Here, we have experimentally evaluated the mirtron origins of three mammalian miRNAs; miR-877, miR-1224 and miR-1226. We have shown these to be a class of splicing-dependent, microprocessor-independent species by using an eGFP model to assess splicing ability and inhibition of RNAi-pathway elements. These data corroborate the confirmed mirtron origin of miRNAs identified and demonstrated in *C. elegans* and *D. melanogaster* (1,2). Interestingly, we show that mirtrons have a variable dependence on Exportin-5 and/or Dicer after forming a pre-miRNA-like hairpin, with miR-1224 unaffected by a competitive inhibitor of downstream RNAi pathway elements. Lastly, we show that seed-matched targets can be silenced by miR-877 in a similar manner to canonical miRNAs, and that mRNA-encoding FXR2, an RNA-binding protein that acts as a regulator of translation (24), can be reduced by miR-877 in the neuronal SH-SY5Y cell line.

Splicing-dependence was confirmed for mirtron precursors of miR-877, miR-1224 and miR-1226 by showing that changes to regulatory splicing motifs present in these hairpins could abrogate splicing, while the silencing ability of putatively spliced U6-transcribed pre-miRNA

equivalents was unaffected. Interestingly, small-RNA hybridization experiments point to low or un-detectable levels of splicing-dependent pre-miRNA precursors for miR-877 and miR-1224. This is despite high levels of host transcript expression and comparable levels of silencing to U6-transcribed pre-miRNA controls that were shown to be expressed in relative abundance. Similarly, qRT–PCR confirmed that low levels of endogenous miR-877 guide strands are present in SH-SY5Y cells, and further that ectopic mirt-miR-877 expression had only a modest effect on mature miR-877 guide strand levels despite substantial eGFP host transcript expression. Together this suggests mirtron biogenesis could be regulated during splicing to limit accumulation of RNAi precursors, a feature which may have functional significance in protecting cells from saturation of the miRNA pathway (13,14). Further, failure to pick up processed guide strands in the small-RNA hybridization experiments, despite precursor detection of U6-transcribed pre-miRNA controls, points towards inefficient processing of these hairpins and may reflect a more recent evolutionary history than canonical miRNAs.

All three mirtrons were additionally unaffected by Drosha knockdown, while reduced silencing ability for both pri-miR-30 and pri-miR-122 mimics demonstrates Drosha dependence of these miRNAs. It is known that the miRNA pathway can be overloaded (13) with Drosha processing appearing to be a rate-limiting step (14). In this regard, it is tempting to speculate that a higher capacity biological processing system other than microprocessor activity could have become a necessity for certain miRNAs with crucial roles in development or normal physiology (5). Alternatively, the specific recognition signals for microprocessor processing may be prohibitive for new miRNAs to have evolved from intronic sequences, while the mirtron pathway offers a less constrained route for short introns to have rapidly evolved into miRNAs. Indeed, this is supported by restriction of all reported mirtrons to either distinct invertebrate or mammalian orders, in contrast, to several canonical miRNAs that show more extensive species conservation (4,25). This may additionally explain the apparent reduced dependence of miR-1224 on downstream RNAi processing elements that were shown by saturation of both Exportin-5 and Dicer with a viral inhibitor of both these proteins (10).

Lastly, FXR2 has been identified as a possible target of miR-877 in a neuronal cell model. Specifically, a reduction in FXR2 mRNA expression levels was seen when a 4.8-fold increase in miR-877 guide strand was induced by ectopic expression of miR-877, although a reduction in FXR2 remains to be confirmed at the protein level to in order to validate this as a target for miR-877. FXR2 is an RNA-binding protein which has functional overlap as a regulator of translation with the Fragile-X mental retardation 1 (FMR1) gene that is mutated or absent in FMR (24,26). Meanwhile, the ABCF1 gene that hosts the miR-877 intron has been shown to have a role in the initiation of translation through interactions with eukaryotic initiation factor 2 (27), potentially placing it in the same biological pathway as FXR2. Further confirmation will be required of this mirtron: target interaction in future through other methods which block the endogenous miRNAs activity. To date, this has been hampered by ineffective blockade of miR-877 activity using both a U6 transcribed sponge sequence and a chemically stabilized antagomir which target the silencing ability of miR-877. However, this may be achievable in future through the use of steric block antisense oligonucleotides to block the biogenesis of miR-877 at the level of splicing (28).

In summary, the work presented here provides experimental verification for the existence of splicing-dependent miRNAs within the mammalian genome. This raises questions for future research regarding the function of this pathway, the regulation of miRNAs generated via splicing, and whether the expression of human mirtrons, which presently represent ~1–2% of all annotated human miRNAs (13/940), are differentially expressed in certain pathologies as seen with canonical miRNAs (29). Unfortunately, the study of mirtrons is likely to be hampered by the low abundance of mirtron transcripts as identified by deep sequencing (4) and our work. However, the development of artificial mirtron expression systems may be able to shed more light on the endogenous function of these mirtrons. Finally, splicing-dependent biogenesis represents a novel entry point into the RNAi pathway that could be exploited synthetically with potential advantages including Drosha independence and tight regulation of mature miRNA species generation.

SUPPLEMENTARY DATA

Supplementary Data are available at NAR Online.

ACKNOWLEDGEMENTS

C.R.S., Y.S., M.S.W. and M.J.A.W. designed the experiments. C.R.S. and Y.S. performed the experiments with contributions from K.D., S.E.A. and S.S. C.R.S., Y.S., M.S.W. and M.J.A.W. wrote the article.

FUNDING

Medical Research Council Studentship (to C.R.S.); A*STAR scholarship (to Y.S.); Swedish Society of Medical Research fellowship (to S.E.A.); Oppenheimer Trust and National Research Foundation (South Africa) (to M.S.W.); Medical Research Council and Parkinson's UK (to M.J.A.W.). Funding for open access charge: Medical Research Council, UK.

Conflict of interest statement. None declared.

REFERENCES

1. Ruby,J.G., Jan,C.H. and Bartel,D.P. (2007) Intronic microRNA precursors that bypass Drosha processing. *Nature*, **448**, 83–86.
2. Okamura,K., Hagen,J.W., Duan,H., Tyler,D.M. and Lai,E.C. (2007) The mirtron pathway generates microRNA-class regulatory RNAs in Drosophila. *Cell*, **130**, 89–100.
3. Han,J., Lee,Y., Yeom,K.H., Nam,J.W., Heo,I., Rhee,J.K., Sohn,S.Y., Cho,Y., Zhang,B.T. and Kim,V.N. (2006) Molecular

basis for the recognition of primary microRNAs by the Drosha-DGCR8 complex. *Cell*, **125**, 887–901.
4. Berezikov,E., Chung,W., Willis,J., Cuppen,E. and Lai,E.C. (2007) Mammalian mirtron genes. *Mol. Cell*, **28**, 328–336.
5. Babiarz,J.E., Ruby,J.G., Wang,Y., Bartel,D.P. and Blelloch,R. (2008) Mouse ES cells express endogenous shRNAs, siRNAs, and other microprocessor-independent, dicer-dependent small RNAs. *Genes Dev.*, **22**, 2773–2785.
6. González-González,E., López-Casas,P.P. and del Mazo,J. (2008) The expression patterns of genes involved in the RNAi pathways are tissue-dependent and differ in the germ and somatic cells of mouse testis. *Biochim. Biophys. Acta*, **1779**, 306–311.
7. Shin,K., Wall,E., Zavzavadjian,J.R., Santat,L.A., Liu,J., Hwang,J., Rebres,R., Roach,T., Seaman,W., Simon,M.I. *et al.* (2006) A single lentiviral vector platform for microRNA-based conditional RNA interference and coordinated transgene expression. *Proc. Natl Acad. Sci. USA*, **103**, 13759–13764.
8. Ely,A., Naidoo,T., Mufamadi,S., Crowther,C. and Arbuthnot,P. (2008) Expressed anti-HBV primary microRNA shuttles inhibit viral replication efficiently in vitro and in vivo. *Mol. Ther.*, **16**, 1105–1112.
9. Han,J., Pedersen,J.S., Kwon,S.C., Belair,C.D., Kim,Y., Yeom,K., Yang,W., Haussler,D., Blelloch,R. and Kim,V.N. (2009) Posttranscriptional crossregulation between Drosha and DGCR8. *Cell*, **136**, 75–84.
10. Lu,S. and Cullen,B.R. (2004) Adenovirus VA1 noncoding RNA can inhibit small interfering RNA and microRNA biogenesis. *J. Virol.*, **78**, 12868–12876.
11. Schellenberg,M.J., Ritchie,D.B. and MacMillan,A.M. (2008) Pre-mRNA splicing: a complex picture in higher definition. *Trends Biochem. Sci.*, **33**, 243–246.
12. Chiang,H.R., Schoenfeld,L.W., Ruby,J.G., Auyeung,V.C., Spies,N., Baek,D., Johnston,W.K., Russ,C., Luo,S., Babiarz,J.E. *et al.* (2010) Mammalian microRNAs: experimental evaluation of novel and previously annotated genes. *Genes Dev.*, **24**, 992–1009.
13. Grimm,D., Streetz,K.L., Jopling,C.L., Storm,T.A., Pandey,K., Davis,C.R., Marion,P., Salazar,F. and Kay,M.A. (2006) Fatality in mice due to oversaturation of cellular microRNA/short hairpin RNA pathways. *Nature*, **441**, 537–541.
14. McBride,J.L., Boudreau,R., Harper,S.Q., Staber,P.D., Monteys,A.M., Martins,I., Gilmore,B.L., Burstein,H., Peluso,R.W., Polisky,B. *et al.* (2008) Artificial miRNAs mitigate shRNA-mediated toxicity in the brain: implications for the therapeutic development of RNAi. *Proc. Natl Acad. Sci. USA*, **105**, 5868–5873.
15. Aagaard,L., Amarzguioui,M., Sun,G., Santos,L.C., Ehsani,A., Prydz,H. and Rossi,J. (2007) A facile lentiviral vector system for expression of doxycycline-inducible shRNAs: knockdown of the pre-miRNA processing enzyme Drosha. *Mol. Ther*, **15**, 938–945.
16. Lund,E. and Dahlberg,J.E. (2006) Substrate selectivity of exportin 5 and dicer in the biogenesis of microRNAs. *Cold Spring Harb. Symp. Quant. Biol.*, **71**, 59–66.
17. Lima,W.F., Murray,H., Nichols,J.G., Wu,H., Sun,H., Prakash,T.P., Berdeja,A.R., Gaus,H.J. and Crooke,S.T. (2009) Human Dicer binds short single-strand and double-strand RNA with high affinity and interacts with different regions of the nucleic acids. *J. Biol. Chem.*, **284**, 2535–2548.
18. O'Malley,R.P., Mariano,T.M., Siekierka,J. and Mathews,M.B. (1986) A mechanism for the control of protein synthesis by adenovirus VA RNAI. *Cell*, **44**, 391–400.
19. Staege,M.S., Hutter,C., Neumann,I., Foja,S., Hattenhorst,U.E., Hansen,G., Afar,D. and Burdach,S.E.G. (2004) DNA microarrays reveal relationship of Ewing family tumors to both endothelial and fetal neural crest-derived cells and define novel targets. *Cancer Res.*, **64**, 8213–8221.
20. Landgraf,P., Rusu,M., Sheridan,R., Sewer,A., Iovino,N., Aravin,A., Pfeffer,S., Rice,A., Kamphorst,A.O., Landthaler,M. *et al.* (2007) A mammalian microRNA expression atlas based on small RNA library sequencing. *Cell*, **129**, 1401–1414.
21. Guo,H., Ingolia,N.T., Weissman,J.S. and Bartel,D.P. (2010) Mammalian microRNAs predominantly act to decrease target mRNA levels. *Nature*, **466**, 835–840.
22. Cheloufi,S., Dos Santos,C.O., Chong,M.M.W. and Hannon,G.J. (2010) A dicer-independent miRNA biogenesis pathway that requires Ago catalysis. *Nature*, **465**, 584–589.
23. Ender,C., Krek,A., Friedlander,M.R., Beitzinger,M., Weinmann,L., Chen,W., Pfeffer,S., Rajewsky,N. and Meister,G. (2008) A human snoRNA with microRNA-like functions. *Mol. Cell*, **32**, 519–528.
24. Siomi,M.C., Zhang,Y., Siomi,H. and Dreyfuss,G. (1996) Specific sequences in the fragile X syndrome protein FMR1 and the FXR proteins mediate their binding to 60S ribosomal subunits and the interactions among them. *Mol. Cell. Biol.*, **16**, 3825–3832.
25. Ibáñez-Ventoso,C., Vora,M. and Driscoll,M. (2008) Sequence relationships among C. elegans, D. melanogaster and human microRNAs highlight the extensive conservation of microRNAs in biology. *PLoS ONE*, **3**, e2818.
26. Darnell,J.C., Fraser,C.E., Mostovetsky,O. and Darnell,R.B. (2009) Discrimination of common and unique RNA-binding activities among fragile X mental retardation protein paralogs. *Hum. Mol. Genet.*, **18**, 3164–3177.
27. Paytubi,S., Wang,X., Lam,Y.W., Izquierdo,L., Hunter,M.J., Jan,E., Hundal,H.S. and Proud,C.G. (2009) ABC50 promotes translation initiation in mammalian cells. *J. Biol. Chem.*, **284**, 24061–24073.
28. Abes,S., Tuner,J.J., Ivanova,G.D., Owen,D., Williams,D., Arzumanov,A., Clair,P., Gait,M. and Lebleu,B. (2007) Efficient splicing correction by PNA conjugation to an R6-penetratin delivery peptide. *Nucleic Acids Res.*, **35**, 4495–4502.
29. Erson,A.E. and Petty,E.M. (2008) MicroRNAs in development and disease. *Clin. Genet.*, **74**, 296–306.